

Supporting information

Nanoparticles-free magnetic mesoporous silica with magneto-responsive surfactants

Sanghoon Kim, Christine Bellouard, Andreea Pasc*, Emmanuel Lamouroux, Jean-Luc Blin, Cédric Carteret, Yves Fort, Mélanie Emo, Pierrick Durand and Marie-José Stébé

1. Preparation and characterisation of CTAF

1.1. Synthesis

Cetyltrimethylammonium bromide (CTAB) was purchased from Merck. Iron (III) chloride (FeCl_3) was purchased from Alfa Aesar. All reagents were used without further purification. **CTAF** was synthesized by adding 1 eq. of iron (III) chloride and 1 eq. of CTAB in methanol. Then, the solution was heated to reflux overnight. The solvent was evaporated and the surfactant was dried *in vacuo* at 60°C for 4 h. The surfactant was characterized using elemental analysis, UV-Vis spectroscopy and differential scanning calorimetry (DSC).

1.2. Elemental analysis of CTAF

Element	% C	% H	% N
Theoretical content	43.30	8.04	2.66
Experimental content	43.70 ± 0.22	7.86 ± 0.35	2.96 ± 0.08

1.3. UV-Vis spectroscopy

The UV-Visible absorbance spectrum was measured with Varian Cary 50 UV-Visible Spectrophotometer in acetonitrile. **CTAF** showed bands for the $[\text{FeCl}_3\text{Br}]^-$ ion similar to those for the $[\text{FeBr}_4]^-$ ion.¹

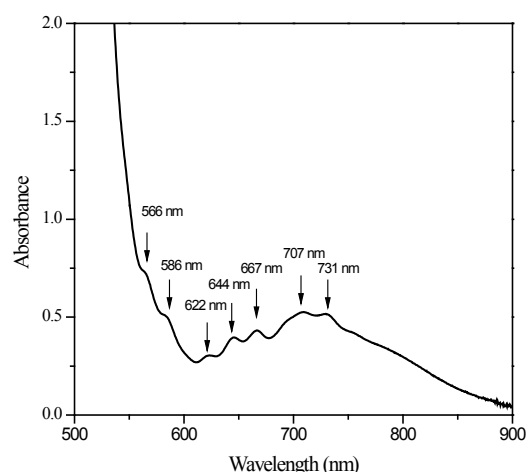


Figure SI1. UV-Visible spectra of CTAF (0.1 M in acetonitrile).

1.4. Differential Scanning Calorimetry

The melting point of CTAF is 64°C, as determined by differential scanning calorimetry (DSC). DSC measurements were performed using a Mettler Toledo DSC1 equipped with a HSS8 sensor under nitrogen flow, with an aluminum crucible (40 mL) at various heating/cooling rates.

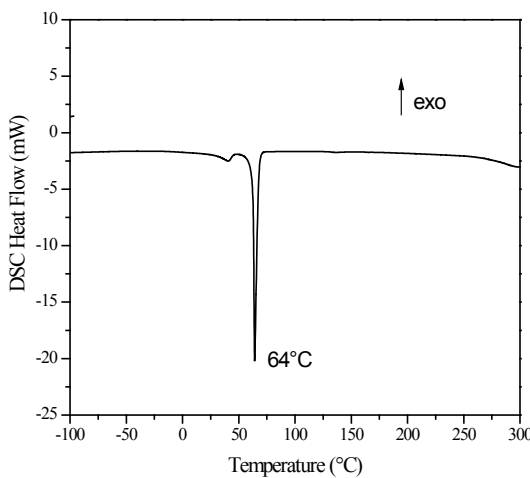


Figure SI2. DSC measurement of magnetic surfactant CTAF

1.5. Phase diagram

The phase diagram was established by preparing samples over the whole range of surfactant/water compositions. The required amounts of the components were weighted in small glass tubes. The homogenization of the samples was achieved by mixing with a vortex stirrer, combined with heat and ultrasounds, whenever necessary. The samples were placed in a thermostatic bath and they were allowed to stand from a few hours to several days at the temperature of interest in order to reach equilibrium. The phases were identified by visual inspection with a polarizing light microscope (Olympus BX 50). The boundary lines of the hydrated crystal domains were determined by Small Angle X-ray Scattering (SAXS) experiments.

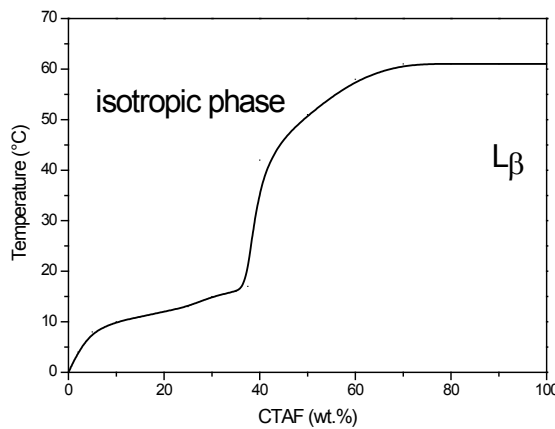


Figure SI3. Concentration-temperature phase diagram of CTAF-water system.

SAXS experiments were performed on a SAXSess mc² instrument (Anton Paar), using line-collimation system. This instrument is attached to a ID 3003 laboratory X-Ray generator (General Electric) equipped with a sealed X-Ray tube (PANalytical, $\lambda_{\text{Cu K}\alpha} = 0.1542 \text{ nm}$) operating at 40 kV and 50 mA. A multilayer mirror and a block collimator provide a monochromatic primary beam. A translucent beam stop allows the measurement of an attenuated primary beam at $q=0$. Samples were put in a paste cell (for hydrated crystals), in a Quartz capillary (for micellar solutions) or between two sheets of Kapton® (for solids) before being placed, at the desired temperature, inside an evacuated sample chamber equipped with a temperature-controlled sample holder unit (TCS 120, Anton Paar), and exposed to X-Ray beam for about

5 min (for solids) or about 60 min (for micelles). Scattering of X-Ray beam was registered by a CCD detector (Princeton Instruments, 2084 x 2084 pixels array with $24 \times 24 \mu\text{m}^2$ pixel size), placed at 309 mm distance from sample. Using SAXSQuant software (Anton Paar), the 2D image was integrated into one-dimensional scattering intensities $I(q)$ as a function of the magnitude of the scattering vector $q = (4\pi/\lambda) \sin(\theta)$, where 2θ is the scattering angle. All data were calibrated by normalizing the attenuated primary beam before being corrected for the background scattering from the cell (and the solvent when necessary) and for slit-smearing effects by a desmearing procedure from SAXSQuant software using Lake method. Using water as a standard, data were converted into absolute scale.

1.6. SAXS analysis of micelles

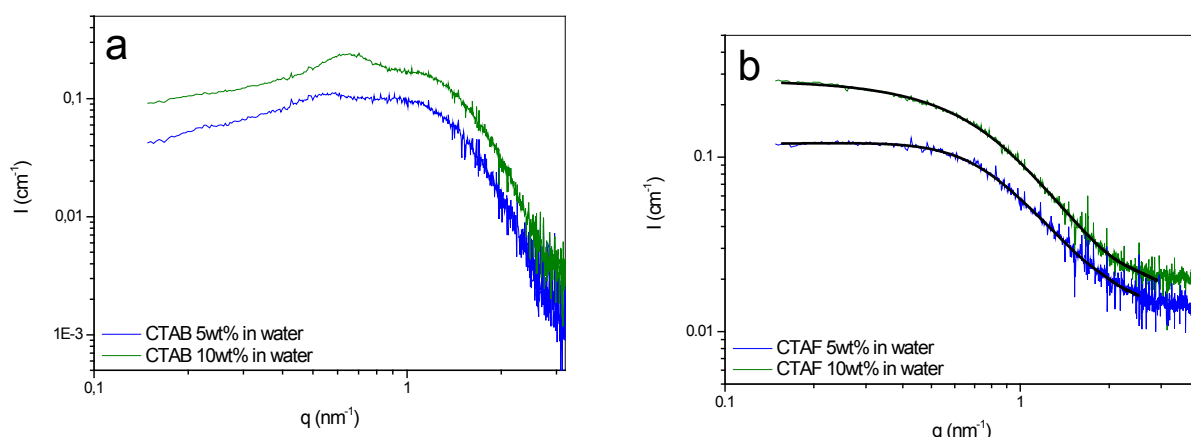


Figure SI4. SAXS patterns of 5 and 10 wt% CTAB in water at 25°C (a) and of 5 and 10 wt% CTAF in water at 25°C (b) in log-log representation

SAXS measurements were performed on 5 and 10 wt% aqueous solutions of parent surfactant, CTAB, and of magnetic surfactant, CTAF. At the same concentration the scattering curves are different on the entire range of q values. Regarding the curves obtained with CTAB solutions, the intensity is proportional to the dispersed volume fraction for all q values (superposition not shown). The presence of an interaction peak at 0.55 nm^{-1} and the strong decrease of the scattered intensity at low q suggest that the structure factor contributes to the scattering of the 5 wt% CTAB solutions. At 10 wt%, the interaction peak is even more pronounced and shifted to higher q values, as expected. For CTAF samples, the SAXS profiles are entirely different. The obtained curves do not present any interaction peaks, suggesting that the iron inhibits interactions between particles. This phenomenon was already reported on similar surfactants.²

1.6. Dynamic light scattering

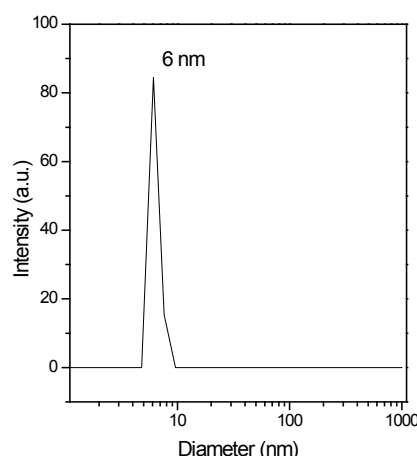


Figure SI5. DLS measurement of 1M CTAF in water

Dynamic light scattering (DLS) experiments were performed with a Malvern 300HSA Zetasizer instrument.

2. Preparation and characterisation of CTAF@SiO₂ materials

Silica materials were prepared by sol-gel, through the cooperative templating mechanism, from micelles of CTAF and tetramethoxysilane (TMOS) as inorganic precursor.

In a typical procedure, 123 mg of CTAF were added in 8 mL of 2 M HCl. Then, 296 mg of tetramethyl orthosilicate (TMOS) were added at room temperature and the mixture was stirred for 30 min. The final molar composition of the gel is 1 SiO₂: 0.12 CTAF: 228 H₂O: 8.2 HCl. Then, the mixture was transferred to a Teflon bottle placed in a stainless-steel autoclave at 343 K for 48 h. The resulting product is filtered on a Buchner funnel and dried in air for 24 h. Before characterization of the silica framework, the surfactant was removed by extraction with ethanol in a Soxhlet during 24 h.

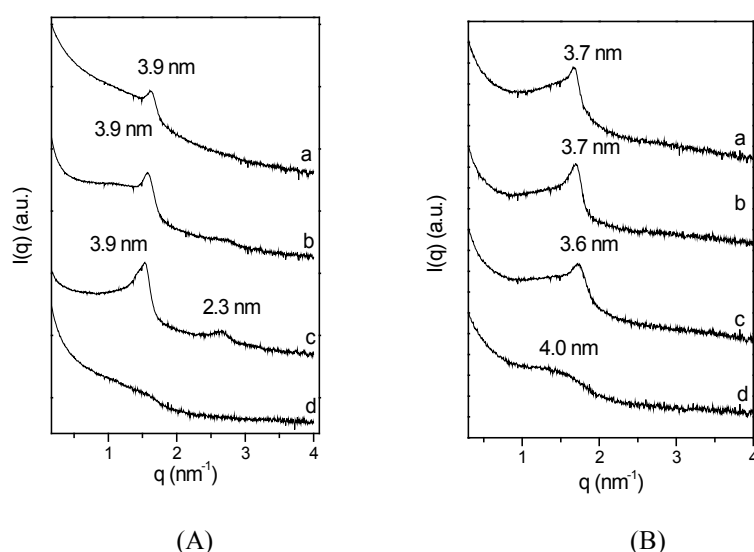


Figure SI6. SAXS data of mesoporous materials prepared by a hydrothermal treatment at 100°C (A), 70°C (B) at a molar ratio surfactant/TMOS of 0.12 and 15 wt% (a), 10 wt% (b), 2.5 wt% (c), 1.5 wt% (d) of CTAF in a solution of 1M HCl. The reactions duration was 24 h.

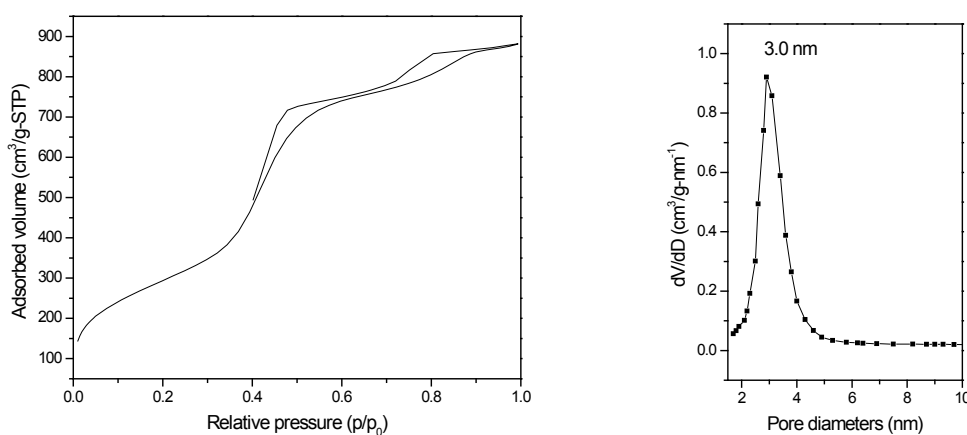


Figure SI7. Nitrogen adsorption/desorption isotherms (left) and the pore diameter (right) of silica materials prepared from 2.5 wt% CTAF in 1 M HCl with R 0.12 and a hydrothermal treatment at 100 °C for 24 h.

In order to optimize the reaction conditions and to obtain ordered silica mesopores, different parameters were modified (pH, temperature and duration of the hydrothermal treatment, surfactant concentration and

molar ratio between the surfactant and the silica precursor). All the reactions were carried out in acidic conditions (pH 0) in order to avoid the precipitation of iron hydroxide. Initially, the surfactant/TMOS molar ratio (R) and the concentration of HCl were fixed at 0.12 and 1M, respectively, values which are similar to those used for the synthesis of MCM41 with CTAB in acidic conditions³. In these conditions, the concentration of surfactant (1.5-15wt%) and the temperature of the hydrothermal treatment (70, 100°C) were varied, while the duration was kept constant of 24 h. Looking at the SAXS patterns of the obtained materials only a single broad peak is observed for most of the materials. This indicates the formation of a wormhole-like structure, with an interpore distance of about 3.9 nm. In these conditions, the better organisation of the silica was obtained at 100°C and 2.5 wt% of **CTAF**, since two reflections at 3.9 and 2.3 nm (ratio 1: $\sqrt{3}$) are observed on the SAXS pattern (Figure SI6A-c). A type IV isotherm characteristic of mesoporous materials was obtained by nitrogen adsorption-desorption analysis. The isotherm exhibits hysteresis characteristic of pore neck. The pore size distribution is rather narrow and its maximum is centred at 3.0 nm (Figure SI7). The values of the specific surface area and pore volume are equal to 1089 m²/g and 1.3 cm³/g, respectively.

Further, we investigated the mesostructuring of porous silica with a higher concentration of HCl (2M) as reaction media. The hydrothermal treatment was performed at 70°C for 24 h and R was varied from 0.08, to 0.12 and to 0.16. In this conditions and for a surfactant concentration of 2.5 wt%, which was to be optimal in the first series of experiments at 1M HCl, the SAXS patterns show that the recovered materials are better organized since 2 reflections observed at 4 and 2.3 nm are narrowest than those of the materials obtained with 1M HCl (Fig. SI8a-c). The results are similar for 1.5wt%, except for R 0.12 were three reflections indexing for a hexagonal network were observed (see manuscript). For all materials, nitrogen adsorption-desorption isotherms are of type IV and the calculated pore size are centred on 2.4-2.7 nm. At both surfactant concentrations, for R 0.08, the silica has necked pores, and a surface area and a pore volume significantly lower than for the materials obtained at R 0.12 and 0.16. The values of the porosity parameters are given in Table SI1.

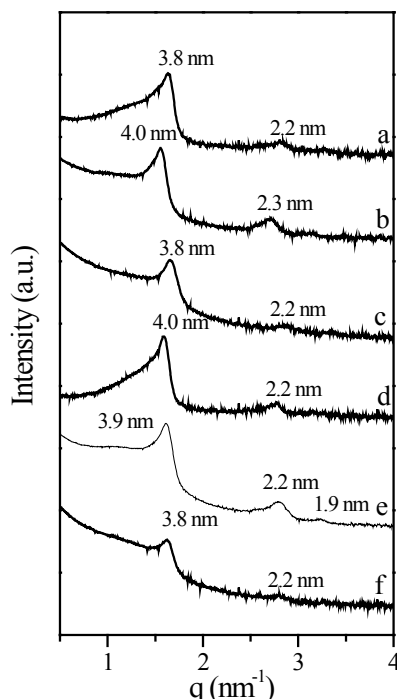


Figure SI8. SAXS data of mesoporous materials prepared with either 2.5 wt% **CTAF** and R of 0.16 (a), 0.12 (b), 0.08 (c) or with 1.5 wt% **CTAF** and R of 0.16 (d), 0.12 (e) and 0.08 (f). The reactions were carried out in aqueous solutions of 2 M HCl and a hydrothermal treatment at 70 °C for 24 h.

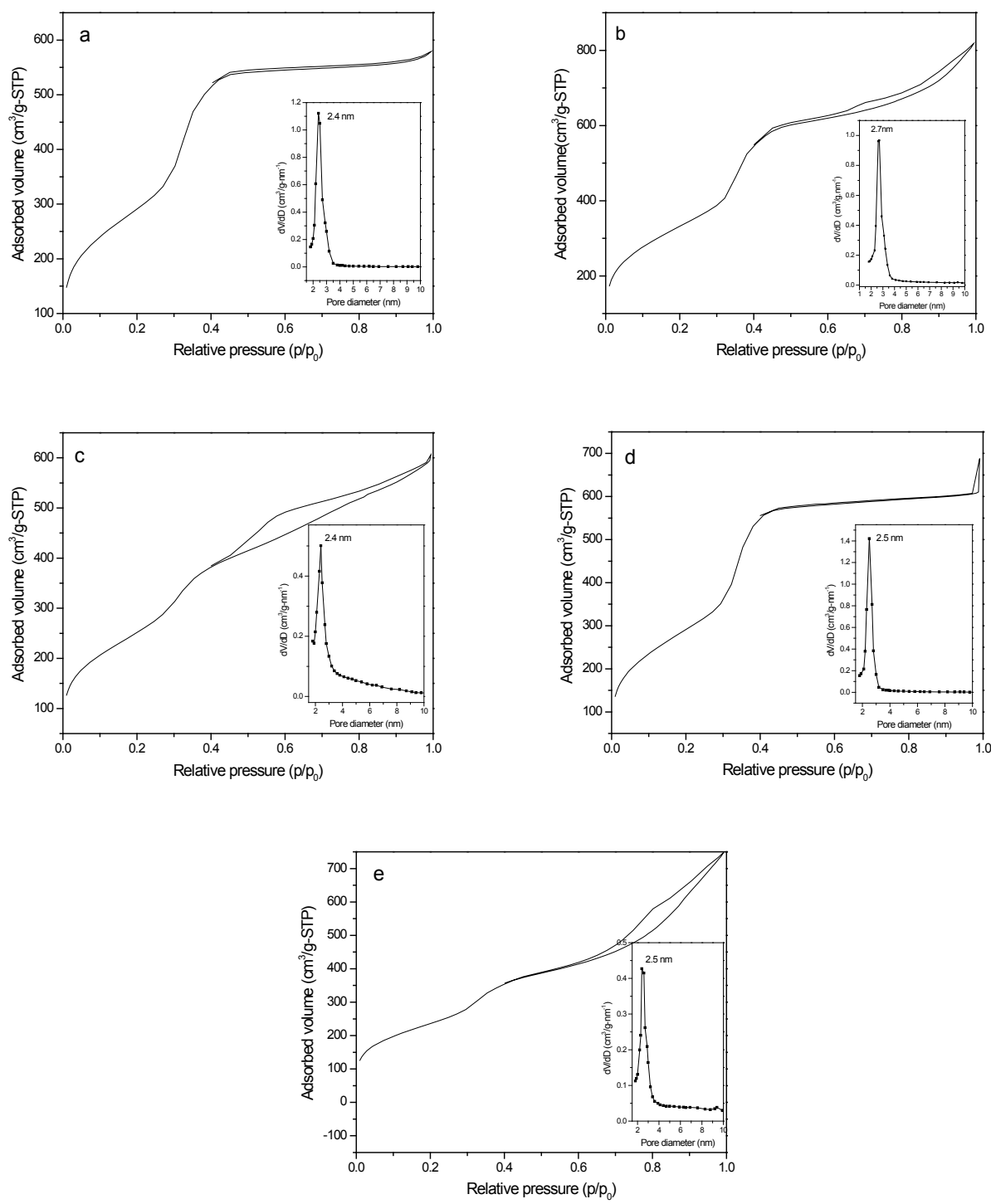


Figure S19. Nitrogen adsorption/desorption isotherms and the pore diameter (insert) of mesoporous silica materials prepared with either 2.5 wt% CTAF and R of 0.16 (a), 0.12 (b), 0.08 (c) or with 1.5 wt% CTAF and R of 0.16 (d), 0.08 (e). The reactions were carried out in aqueous solutions of 2 M HCl and a hydrothermal treatment at 70 °C for 24 h.

Table S11. Summary of the specific area (S_{BET}) and porous volume (V_p) values for the mesoporous silica materials prepared with 2M HCl under a hydrothermal treatment at 70 °C for 24 h.

Reaction conditions	S_{BET} (m^2/g)	V_p (cm^3/g)
2.5 wt% CTAF, R 0.08	937	0.77
2.5 wt% CTAF, R 0.12	1213	1.05
2.5 wt% CTAF, R 0.16	1078	0.76
1.5 wt% CTAF, R 0.08	860	0.99
1.5 wt% CTAF, R 0.16	1096	0.81

Post-synthesis treatment for organized mesoporous ferrisilicates (Fe@SiO₂)

Dry hybrid material (CTAF@SiO₂) was placed in a saturated atmosphere of triethylamine for 5 minutes. The organic templated was washed with hexane, the powder was then heated to 70 °C and washed with absolute ethanol to afford Fe@SiO₂.

Spectroscopic measurements

Diffuse reflectance spectra of powder samples were recorded at room temperature in the 200–650 nm range using a UV-visible-NIR spectrometer (Varian Cary 5000) equipped with an integrating sphere attachment.

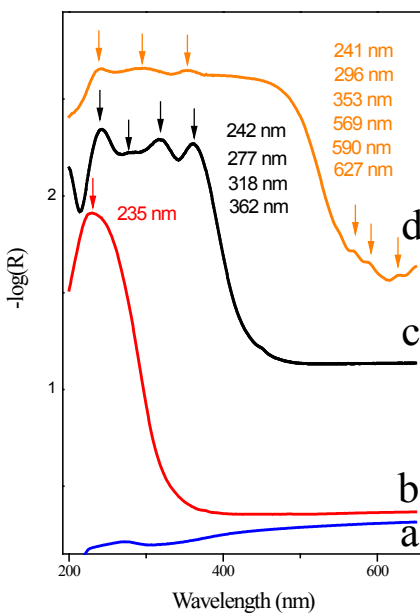


Figure SI10. UV-Visible diffuse reflectance spectra of materials: (a) bare SiO₂, (b) Fe@SiO₂, (c) CTAF@SiO₂ and (d) CTAF

Magnetic measurements

Magnetic measurements were performed with powder samples (CTAF@SiO₂, Fe@SiO₂ and bare silica) placed in a capsule and plastic straw with a PPMS Quantum Design instrument in the 2 K–300 K temperature range and a magnetic field up to 9 T. Raw data have been corrected from the diamagnetic contribution of samples and sample holder.

Fig. SI11 and 12 show the magnetization of the hybrid **CTAF@SiO₂** and **Fe@SiO₂** samples measured at different temperatures and plotted as a function of the ratio of the magnetic field (B) to temperature (T). For both samples, all measurements above 10 K are superimposed, this scaling is the signature of a paramagnetic signal of free ions. The obtained unique curve is well fitted by a Brillouin law⁴ with an S = 5/2 spin. This is exactly the spin value expected for the high spin state of Fe³⁺ ions.

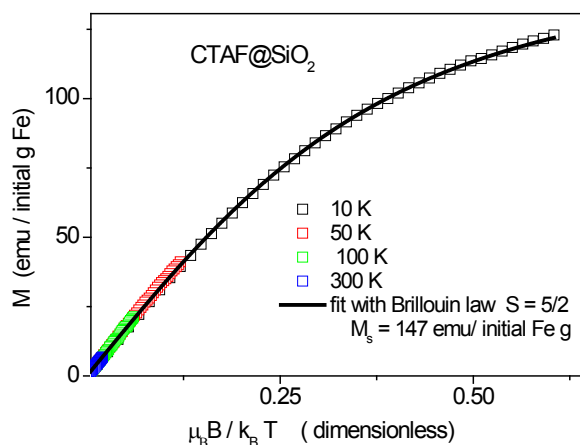


Figure SI11. Magnetization measurements of **CTAF@SiO₂** as a function of the dimensionless parameter $\mu_B B / k_B T$ for $T > 10K$. μ_B is the Bohr magneton, k_B the Boltzmann constant. The straight line is a fit with the Brillouin function with $S = 5/2$.

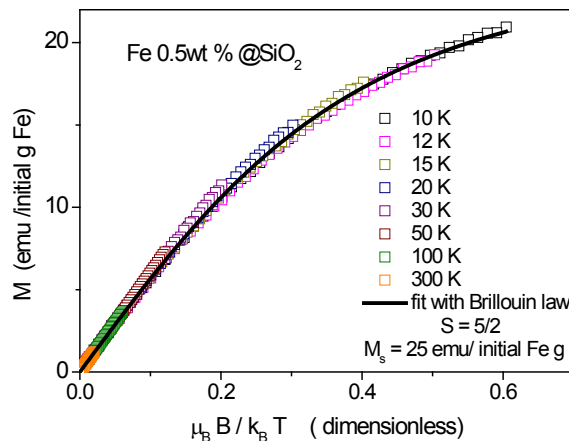


Figure SI12. Magnetization measurements of **Fe@SiO₂** as a function of the dimensionless parameter $\mu_B B / k_B T$ for $T > 10K$. μ_B is the Bohr magneton, k_B the Boltzmann constant. The straight line is a fit with the Brillouin function with $S = 5/2$.

Calculation of the iron weight content.

For **CTAF@SiO₂** material, the initial theoretical amount of Fe is 5wt%, while the measured amount resulting from magnetic measurements is then: $0.05 * 147 / 500 = 1.47 \text{ wt\%}$ which was roughly estimated to 1.5 wt%. For **Fe@SiO₂** material described in Figure 4, the initial theoretical amount of Fe is 9.55 w%, the measured amount resulting from magnetic measurements is then : $0.0955 * 25 / 500 = 0.47 \text{ wt\%}$ or roughly 0.5 wt%.

¹ M. Dobbelin, V. Jovanovski, I. Llarena, L. J. Claros Marfil, G. Cabanero, J. Rodriguez, D. Mecerreyres, *Polym. Chem.* **2011**, *2*, 1275.

-
- ² P. Brown, A. Bushmelev, C. P. Butts, J. Cheng, J. Eastoe, I. Grillo, R. K. Heenan and A. M. Schmidt, *Angew. Chem. Int. Ed.* **2012**, *51*, 2414-2416.
- ³ Q. Huo, D. I. Margolese, and G. D. Stucky *Chem. Mater.* **1996**, *8*, 1147-1160
- ⁴ Introduction to solid state physics. 7th edition, C. Kittel, The University of California at Berkeley ISBN: 0-471-11181-3.